IEEE Access
Multidisciplinary | Rapid Review | Open Access Journal

Received September 4, 2019, accepted November 8, 2019, date of publication November 12, 2019, date of current version December 4, 2019.

Digital Object Identifier 10.1109/ACCESS.2019.2953142

Statistical Characterization of GNSS Signal-in-Space Ranging Errors for the User Within and Beyond Space Service Volume

YIFAN ZHOU, YUEKE WANG, WENDE HUANG, AND LEYUAN SUN
College of Intelligence Science and Technology, National University of Defense Technology, Changsha 410073, China
Corresponding author: Yueke Wang (wyk_cs@sina.com)

This work was supported by the State Key Laboratory of Geo-Information Engineering, under Grant SKLGIE2018-Z-1-2.

ABSTRACT The number and scope of space applications of global navigation satellite systems have grown significantly. However, the availability and the navigation performance for a spacecraft operating within and beyond the space services volume are different from those of terrestrial service volume users. To effectively evaluate the space service performance of navigation satellite systems, we present the calculation method of signal-in-space ranging error for space users. Considering the geometric visibility and the constraints of the lowest carrier-to-noise ratio, we analyze the feasibility of receiving the signal transmitted from the different off-nadir angles and obtain the coverage area of navigation satellite. Then, the relationship between the weighting factors of ephemeris errors and the orbital height of the user spacecraft is analyzed. Finally, the statistics characteristic of signal-in-space ranging error of typical navigation satellites is presented. The results show that the signal-in-space ranging error increases first and then decreases as the orbital height of the user increases. Generally, when the user's orbital height is slightly higher than the orbital height of the navigation satellite, the signal-in-space ranging error reaches a maximum. In particular, due to the significant horizontal orbit error, global signal-in-space ranging error of the Beidou geostationary orbits satellites increase significantly compared with the user located on the ground. Therefore, the impact of user height changes on the statistical properties of signal-in-space ranging error cannot be ignored when evaluating the navigation performance of the space user.

INDEX TERMS GNSS, SISRE, SSV.

I. INTRODUCTION

As the number of human space exploration missions increases year by year, the autonomous positioning and navigation supported by Global Navigation Satellite System (GNSS) are gradually replacing ground monitoring and control, becoming an indispensable means for spacecraft to navigate autonomously in orbit. Historically, most space users have been located at low altitudes, where GNSS signal reception is similar to that on the ground. However, the use of GNSS has expanded to other orbit regimes like Geostationary Equatorial Orbits (GEO), High Eccentric Orbits (HEO), and even Lunar Orbits (LO).

In a statistical sense, the point location accuracy of GNSS can be described by the product of the User Equivalent Range Error (UERE) and the Dilution Of Precision (DOP), where UERE includes all measurements and modeling error of the pseudorange and DOP map these errors to the position uncertainty. UERE can be further divided into Signal-In-Space Range Errors (SISRE) and User Equipment Errors (UEE). While the UEE term includes all receiver related contributions, such as noise, multipath, and uncorrected atmospheric errors, SISRE describes the statistical uncertainty caused by ephemeris error [1]. As one of the major error sources of pseudorange measurement, SISRE directly affects the positioning accuracy and integrity. Therefore, proper knowledge of the statistical characteristic of SISRE is essential for the performance assessment and satellite selection for a Multi-GNSS context.

For users on earth, the statistical characteristic of SISRE of different satellite navigation systems has been discussed. Chen *et al.* derived calculation formulation of SISRE of different types of Beidou satellites and assessed the SISRE of Beidou satellites for the user on earth [2].

The associate editor coordinating the review of this manuscript and approving it for publication was Seung-Hyun Kong.

Heng *et al.* analyzed long-term stationarity of the SISRE performance of Russia's GLObal NAvigation Satellite System (GLONASS) and characterized the SISRE concerning mean and standard deviation, distribution, the correlation among satellites, and geographic dependency [3]. Oliver Montenbruck *et al.* presented a harmonized framework for the calculation method of multi-GNSS SISRE based on the comparison of broadcast and precise ephemerides. Besides, Montenbruck *et al.* pointed that representative global average Root Mean Square (RMS) SISRE values for the European Union's GALILEO, the United States' Global Positioning System (GPS), the China's second-generation Beidou navigation satellite System (BDS-2), and GLONASS in 2017 are 0.2 m, 0.6 m, 1 m, and 2 m respectively [4].

While Terrestrial Service Volume (TSV) includes all terrestrial and space GNSS users up to an altitude of 3,000 km, the Space Services Volume (SSV) is defined as the region of space between 3,000 km and 36,000 km above the Earth's surface [5]. For the SSV user, the United Nations (UN) sponsored International Committee on GNSS (ICG) is leading the effort to coordinate the development of an interoperable SSV. Using both a coverage grid approach and a suite of example mission profiles, a three-phase joint analysis effort was proposed to characterize single-constellation and combined SSV performance within the SSV [6]. The observation geometry of different orbital inclination and altitude satellites was summarized in [7]. Tang *et al.* presented the application method of the Inter-Satellite Link (ISL) for SSV users and analyzed their service performance [8]. Shehaj *et al.* investigated the effect of different antenna pattern assumptions on the simulated signal availability and the consequent simulated navigation performance of a spaceborne receiver orbiting in a very highly elliptical orbit from the Earth to the Moon [9]. Jing *et al.* characterized the SSV in terms of the four parameters of minimum received power, satellite visibility, pseudorange accuracy, and Geometric Dilution Of Precision (GDOP) [10].

However, in the above analysis of the navigation performance of the space-borne receivers, SISRE still utilizes the same value with the user on the surface of the earth. From the definition of SISRE, SISRE is related to the relative position of GNSS satellites and user spacecraft. The max off-boresight angle of the Medium Earth Orbit (MEO) navigation satellite to the earth is about 13 to 14 degrees, the max off-boresight angle of the GEO navigation satellite and Inclined GeoSynchronous Orbit (IGSO) navigation satellite to the Earth is about 8 degrees. Therefore, the off-boresight angle of the navigation signal received by the ground user is generally not more than 14 degrees. Since space users can even use the side lobe signal of the navigation satellite for navigation, the range of off-boresight angle of the received navigation signal is much larger than the ground user. Therefore, the use of ground SISRE for a space user may be not accurate enough. To better evaluate the performance of spacecraft within and beyond SSV, we analyzed the SISRE statistical characteristics of existing GNSS for spacecraft of different altitudes, and the rest of the paper is structured as follows. The next section presents the definition and calculation method of SISRE. Section III offers the variation trend of weighting factors of space users based on the analysis of the geometric visibility and the Carrier-Noise Ratio (CNR). Section IV shows the SISRE statistical characteristics of typical navigation satellites. Section V contains the conclusions and future work.

II. DEFINITION AND CALCULATION METHOD OF SISRE

The SISRE can be defined as the difference between the actual pseudorange and the pseudorange that has been corrected the ephemeris error, including the orbit error and the clock error. The direction of the SISRE is from the satellite to the user on the ground, also known as the line of sight. The satellite clock error is scalar and can, therefore, be added directly to the SISRE. However, the satellite orbit error is a vector. The satellite orbit error has three directions, namely the radial direction, the along-track direction, and the cross direction. As in Fig. 1, with the center of the earth as the origin, the along-track direction as the x-axis, the cross direction as the y-axis, and the opposite direction of the radial direction as the z-axis, the Cartesian coordinate system OXYZ is established.

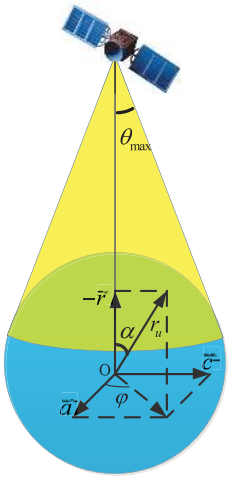

FIGURE 1. Coordinate system diagram.

Suppose the spherical coordinate of the user is (r_u, α, φ), where r_u is the orbital radius of user spacecraft, α is the polar angle, and φ is the azimuthal angle; then the Cartesian coordinates of the user satellite are $X_u = (r_u \sin\alpha\cos\varphi, r_u \sin\alpha \sin\varphi, r_u \cos\alpha)$, and the unit vector of the GNSS satellite pointing to the user's observation vector is

$$\vec{\rho} = \frac{1}{\left|\vec{\rho}\right|}\begin{bmatrix} r_u \sin\alpha\cos\varphi \\ r_u \sin\alpha \sin\varphi \\ r_u \cos\alpha - r_g \end{bmatrix}, \tag{1}$$

where r_g is the orbital radius of the GNSS satellite; $\left|\vec{\rho}\right|$ is the range between the user spacecraft and the GNSS satellite and can be calculated as

$$\left|\vec{\rho}\right| = \sqrt{r_u^2 + r_g^2 - 2r_u r_g \cos\alpha}. \tag{2}$$

Then, the projection coefficients of the orbit error of the along-track direction, the cross direction, and the radial direction are

$$l(X_u) = \frac{r_u \sin\alpha \cos\varphi}{\left|\vec{\rho}\right|}$$
$$m(X_u) = \frac{r_u \sin\alpha \sin\varphi}{\left|\vec{\rho}\right|}$$
$$n(X_u) = \frac{r_g - r_u \cos\alpha}{\left|\vec{\rho}\right|}. \quad (3)$$

Project the ephemeris error to the line of sight and take a first-order approximation, then instantaneous SISRE can be defined as

$$iSISRE = \Delta rn(X_u) - v\Delta t + \Delta al(X_u) + \Delta cm(X_u), \quad (4)$$

where Δa, Δc, and Δr are the orbit error of the cross direction, the along-track direction, and the radial direction, respectively; Δt refers to the clock error and v is the velocity of light.

Since the clock error and orbit error of the satellite is time-varying, the RMS value of SISRE is generally used to evaluate the space service performance [1]. Then, the single-point SISRE can be defined as

$$SISRE = \mathrm{rms}(iSISRE). \quad (5)$$

Since $l(X_u)$, $m(X_u)$ and $n(X_u)$ are the function of the user's location, the single-point SISRE is also a function of the user's location. To obtain a SISRE value that is independent with the user's position, statistical values of the single point SISRE for all user in the coverage region of the satellite was introduced.

The worst single point SISRE within the satellite coverage area can be defined as

$$maxSISRE = \max_{X_u \in \Sigma} (SISRE). \quad (6)$$

Since the satellite coverage area is rotationally symmetric around the line connecting the satellite to the center of the earth, the cross-correlation term in the three directions of orbit error and the correlation between the clock error and the orbit error of the along-track and the cross direction contribute nothing to the global SISRE. Without loss of generality, the global SISRE is defined as the expectation of the single-point SISRE of all users in the area, i.e.

$$globalSISRE = \sqrt{(vT)^2 + w_R R^2 + w_A A^2 + w_C C^2 - 2w_{R,T} v\overline{\Delta t \Delta r}}, \quad (7)$$

where R, A, C, and T denote the RMS of orbit error and clock error; $\overline{\Delta t \Delta r}$ is the expectation of the product of the clock error and the radial orbit error. If both the mean value of the radial orbit error and the clock are zero, $\overline{\Delta t \Delta r}$ is equal to the cross-correlation of the radial orbit error and the clock error.

w_A, w_C, w_R, and $w_{R,T}$ are weighting factors of the ephemeris error and can be calculated as

$$w_A = E[l^2(X_u)] = \iint_{X_u \in \Sigma} l^2(X_u) p(X_u)$$
$$w_C = E[m^2(X_u)] = \iint_{X_u \in \Sigma} m^2(X_u) p(X_u)$$
$$w_R = E[n^2(X_u)] = \iint_{X_u \in \Sigma} n^2(X_u) p(X_u)$$
$$w_{R,T} = E[n(X_u)] = \iint_{X_u \in \Sigma} n(X_u) p(X_u), \quad (8)$$

where Σ is the coverage zone of the navigation satellite; $p(X_u)$ is the probability density function of the user position; w_A is the weighting factor of the orbit error of the along-track direction, which represents the average contribution of the orbit error of the along-track direction to the SISRE; similarly, w_C and w_R represent the weighting factor of orbit error of cross direction and the radial direction, respectively; $w_{R,T}$ represents the weighting factor of the expectation of the product of the radial direction orbit error and the clock error.

Assuming that the user spacecraft are evenly distributed on a geocentric centered sphere, then both $\sin\alpha$ and φ are uniformly distributed [11], and the probability density function of the user position is

$$p(X_u) = p(r_u, \alpha, \varphi) = \frac{r_u^2 \sin\alpha \mathrm{d}\alpha \mathrm{d}\varphi}{S_\Sigma}. \quad (9)$$

where S_Σ is the area of the coverage zone.

Considering that the satellite orbit and the clock difference are generally solved together by the control segment of the GNSS, such as GPS, it is usually believed that the radial direction orbit error and the clock error are negatively correlated [1], [12]. However, BDS uses the Two-Way Satellite Time and Frequency Transfer (TWSTFT) method to determine the satellite clock [12], i.e., the orbit and the clock difference are solved separately, the orbital error sometimes is considered to be uncorrelated with the clock error. In this case, the global SISRE can be defined as

$$globalSISRE' = \sqrt{(vT)^2 + w_R R^2 + w_A A^2 + w_C C^2}. \quad (10)$$

In (7) and (10), for a specific navigation satellite and a user satellite of a particular altitude, the weighting factor is constant. Thus, we only need to calculate the statistical value of the broadcast ephemeris error to determine the statistical characteristics of the SISRE if the weighting factors are known. For the ground users, the corresponding weighting factor has been given [1], but there is still no relevant research for space users. The next section will focus on analyzing the relationship between ephemeris error weighting factors and user height.

III. WEIGHTING FACTORS OF SPACE USER

As in (8), the weighting factor is the geographical mean of the error projection coefficients of the satellite coverage area; thus, the value of the weighting factor is related to the coverage area of the navigation satellite. Navigation satellites typically use directional antennas to transmit navigation signals to the ground; thus, potential users must locate within the conical of the navigation signal and guarantee the navigation signal not blocked by the earth. We define the above conditions as the geometric visibility between the user spacecraft and the navigation satellite. On the other hand, since the onboard receiver can only handle navigation signals with signal strengths above the designed threshold, the coverage area of the satellite is also affected by the signal strength. Thus, the coverage of navigation satellites is determined by the geometric visibility and the received signal strength constraint. We analyze the coverage of navigation satellites for space users and calculate the ephemeris error weighting factors for space users in this section. At first, we summarized the geometric visibility for the user at different heights. Then, the signal feasibility under constraints of receive sensitivity is analyzed. At last, based on the analysis of coverage, we calculated the weighting factors of the typical satellite navigation system in the third part of this section.

A. GEOMETRIC VISIBILITY OF USER SPACECRAFT

As shown in Fig. 2, the coverage area of the GNSS satellite to the ground is a spherical cap, and the spherical crown Σ can be defined as

$$\Sigma = \{X_u(r_u, \alpha, \varphi) | 0 \le \alpha \le \frac{\pi}{2} - \theta_{\max}, 0 \le \varphi \le 2\pi, r_u = r_e\}, \tag{11}$$

where $\theta_{\max} = \arcsin \frac{r_e}{r_g}$ is the max off-nadir angle of which the navigation signal can be received by the user on earth; r_e is the orbital radius of the earth.

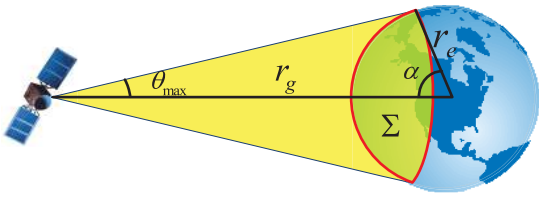

FIGURE 2. Coverage zone for the user on earth.

For space users, navigation satellites have different coverage for the user at different heights. As in Fig. 3, if the cutoff angle of the transmit antenna is less than 90 degrees, coverage region for the user at a certain height can be divided into three types. The user height corresponding to the three coverage types is

$$\begin{cases} \text{Type1}, & r_e \le r_u \le r_g \sin\theta_m \\ \text{Type2}, & r_g \sin\theta_m < r_u < r_g \\ \text{Type3}, & r_u \ge r_g, \end{cases} \tag{12}$$

where θ_m is the cutoff angle of the transmit antenna.

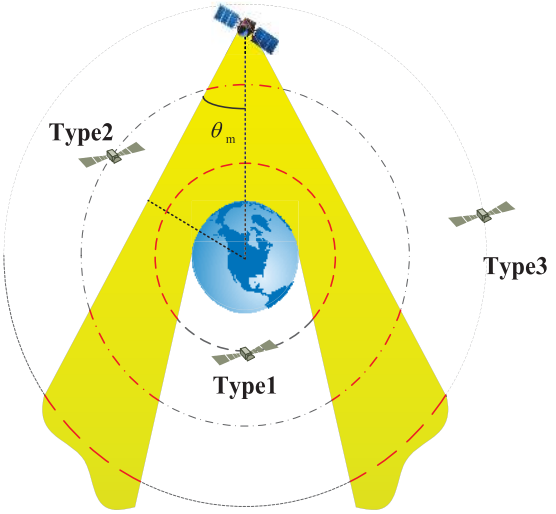

FIGURE 3. Three types of the coverage region.

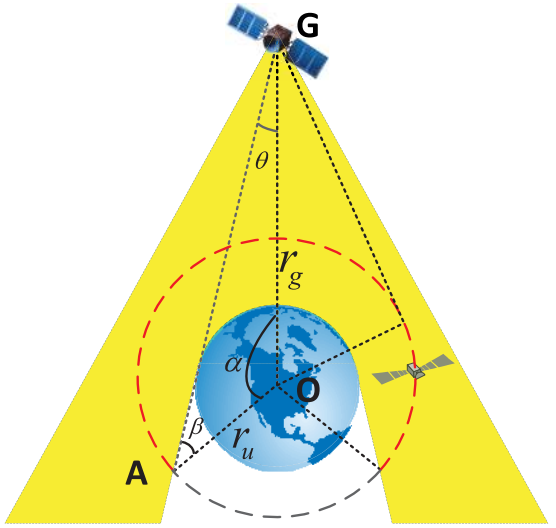

FIGURE 4. Coverage zone of type 1.

Fig. 4 shows the section of the satellite coverage zone of Type1. Rotating the visible area in Fig. 4 (the red dashed arc) around the line connecting the navigation satellite to the center of the earth, we can get the continuous spherical cap surface, i.e., the complete coverage zone. The mathematics definition of the coverage zone Σ for the user at a certain height r_{u0} is

$$\begin{aligned} \Sigma &= \{X_u(r_u, \alpha, \varphi) | 0 \le \alpha \le \alpha_{\max}, 0 \le \varphi \le 2\pi, r_u \equiv r_{u0}\} \\ \alpha_{\max} &= \pi - \arcsin\frac{r_e}{r_u} - \arcsin\frac{r_e}{r_g}. \end{aligned} \tag{13}$$

Here $r_u \equiv r_{u0}$ means the orbital radius of the user is constant. The area of the coverage zone is

$$S_\Sigma = \int_0^{\alpha_{\max}} \int_0^{2\pi} r_u^2 \sin\alpha \, d\alpha \, d\varphi. \tag{14}$$

It is evident that the higher the satellite height, the larger the coverage area is, since $\alpha_{\max}$ increases along with the rise in the height of the user.

Fig. 5 presents the coverage area of Type 2 for the user equipped with both a zenith-pointing antenna and a nadir pointing antenna. The mathematics definition of the coverage zone Σ and the calculation of the area of the coverage zone S_Σ for the user at a certain height r_{u0} are

$$\begin{aligned}
\Sigma &= \{X_u(r_u,\alpha,\varphi)|\alpha\in[0,\alpha_3]\cup[\alpha_2,\alpha_1],\\
&\qquad \varphi\in[0,2\pi],\, r_u\equiv r_{u0}\}\\
S_\Sigma &= \int_0^{\alpha_3}\int_0^{2\pi} r_u^2\sin\alpha\mathrm{d}\alpha\mathrm{d}\varphi + \int_{\alpha_2}^{\alpha_1}\int_0^{2\pi} r_u^2\sin\alpha\mathrm{d}\alpha\mathrm{d}\varphi\\
\alpha_1 &= \pi - \arcsin\frac{r_e}{r_u} - \arcsin\frac{r_e}{r_g}\\
\alpha_2 &= \pi - \theta_m - \arcsin\left(\frac{r_g\sin\theta_m}{r_u}\right)\\
\alpha_3 &= \arcsin\left(\frac{r_g\sin\theta_m}{r_u}\right) - \theta_m, \qquad (15)
\end{aligned}$$

where α_1, α_2, α_3 are the endpoint of the valid interval of α (the polar angle of the spherical coordinate). Since α equals to the geocentric angle between the navigation satellite and the user, α_3 is the max geocentric angle for a zenith-pointing antenna, α_1 and α_2 are the max and min geocentric angle for a nadir-pointing antenna.

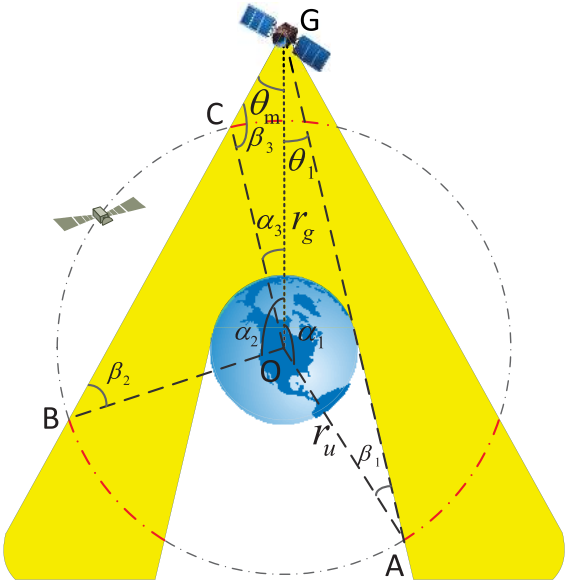

FIGURE 5. Coverage zone of type 2.

In particular, when the cutoff angle of the transmit antenna is 90 degrees, the coverage area directly changes from Type1 to Tpye3 as the user height increases.

As in Fig. 6, when the user satellite is higher than the navigation satellite, the coverage zone for the user at a certain height belongs to Type 3. In this case, space users can only receive signals by the nadir pointing antenna. Besides, as the height of the user increases, the coverage of height decreases.

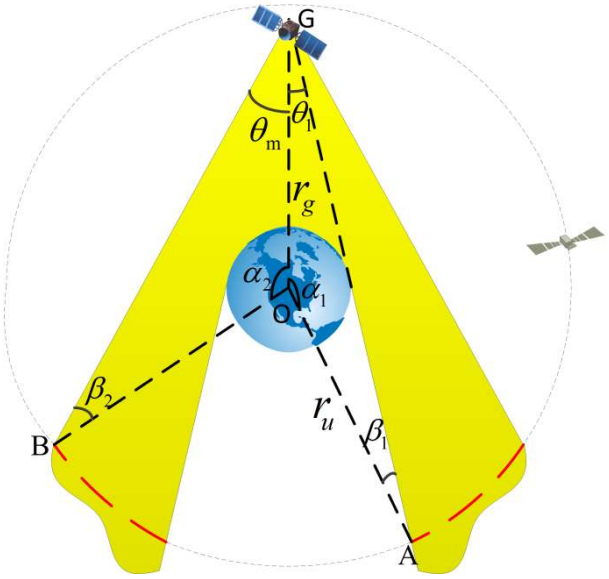

FIGURE 6. Coverage zone of type 3.

The mathematics definition of the coverage zone Σ and the calculation of the area of the coverage area S_Σ are

$$\begin{aligned}
\Sigma &= \{X_u(r_u,\alpha,\varphi)|\alpha\in[\alpha_2,\alpha_1],\varphi\in[0,2\pi],\, r_u\equiv r_{u0}\}\\
S_\Sigma &= \int_{\alpha_2}^{\alpha_1}\int_0^{2\pi} r_u^2\sin\alpha\mathrm{d}\alpha\mathrm{d}\varphi\\
\alpha_1 &= \pi - \arcsin\frac{r_e}{r_u} - \arcsin\frac{r_e}{r_g}\\
\alpha_2 &= \pi - \theta_m - \arcsin\left(\frac{r_g\sin\theta_m}{r_u}\right), \qquad (16)
\end{aligned}$$

where α_1, α_2 are the endpoint of the valid interval of α. Besides, α_1 and α_2 are the max and min geocentric angle between the navigation satellite and the user, respectively.

B. SIGNAL FEASIBILITY UNDER CONSTRAINTS OF RECEIVE SENSITIVITY

The CNR at a GNSS receiver can be expressed by the following formula [10]:

$$C/N_0 = P_t + G_t - L_S - L_a + G_r - L_p - L_{proc} - N_0, \qquad (17)$$

where P_t is the transmitting power of power amplifier, G_t is transmitting antenna gain, L_S is the free space propagation loss, L_a is atmospheric loss and be set as 0 dB in the following simulation, G_r is receiving antenna gain, L_p represents the polarization mismatch loss and be set as 4 dB in the simulation, L_{proc} is the process loss of receiver, N_0 is the noise power spectrum density.

The space propagation loss L_s in free space can be obtained from the expression [13]

$$L_S = 20\log_{10}\left(\frac{4\pi d}{\lambda}\right). \qquad (18)$$

where d is the signal propagation distance and λ is the wavelength of navigation signal.

The process loss L_{proc} derives from three-stage series devices, including Low Noise Amplifiers (LNA), cables, and Radio Frequency (RF) front-ends. Suppose that the LNA has a Noise Factor (NF) of 2 dB and a gain of 26 dB, the loss in the cable is 2.5 dB, and the NF of RF front-end is 9 dB; thus the process loss equals 2.09 dB [10].

The noise power spectrum density can be calculated as [10]

$$N_0 = 10 \log_{10} kT, \tag{19}$$

where k is the Boltzmann constant and T refers to the ambient temperature and was set as 290 K in the simulation.

Although antenna gain patterns of GPS had been given [14], the antenna gain patterns of other navigation systems are still unclear. Fortunately, Parker presented the signal strengths received by GEO user satellites at the edge of the main lobe of different GNSS satellites [15]. Assuming the transmit antenna gain at the edge of main lobe is -5dB and the signal strengths at the edge of the main lobe of different GNSS received by GEO user satellites equal to the value in [15], we calculated the corresponding transmit power and summarized the result in Table 1. In addition, since the original intention of the design of the navigation satellite antenna is to meet the needs of the ground users, the navigation signal strength generally begins to drop sharply near the edge of the earth. Furthermore, although there are specific differences, we assumed that the main trends of the gain of different satellite transmitting antennas with the nadir angle are generally the same, that is, as the nadir angle becomes larger, the transmit antenna gain becomes smaller. BDS employs a mixed constellation of MEO, IGSO, and GEO satellites. Considering that the orbital altitude of the IGSO satellite is the same as that of the GEO satellite, we assumed that the antenna pattern and transmitter power of IGSO and GEO satellites are the same. With these assumptions, we calculated the transmit antenna pattern of typical navigation satellites in Fig. 7.

TABLE 1. SSV signal characteristics for each GNSS service provider.

Satellite name	GPS [a]	GLO [b]	Gal [c]	BD M [d]	BD G/I [e]
Orbit radius (km)	26560	25440	29600	27900	42157
Signal	L1	L1	E1	B1	B1
Frequency (MHz)	1575.42	1605.375	1575.42	1561.098	1561.098
Transmit Power (dBW)	17.65	22.57	19.60	17.45	17.43
Earth blocked angle(°)	13.88	14.50	12.43	13.20	8.69
Reference off-nadir angle(°) [15]	23.5	26	20.5	25	19
Minimum signal power for GEO user (dBW) [15]	-184	-179	-182.5	-184.2	-185.9

[a] GPS IIR-M [b] GLONASS [c] GALILEO [d] Beidou MEO [e] Beidou GEO/IGSO

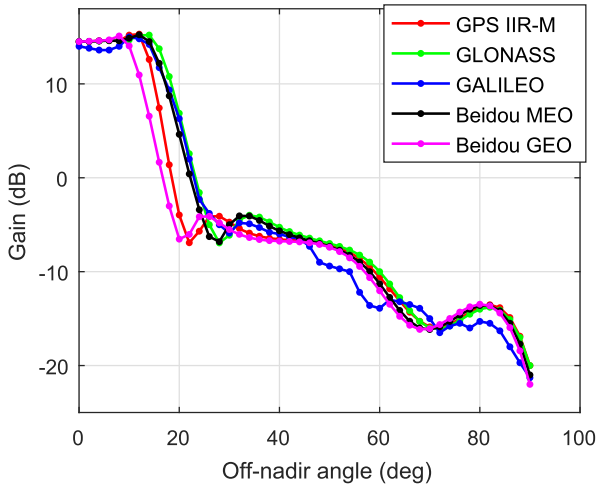

FIGURE 7. Assumed gain patterns of the antennas used in the simulation. The GPS antenna gain pattern is based upon the data in [14].

We sampled the space region from the Earth's surface to a height of 60 times the Earth's radius, with a sampling interval of 1000 km for the orbital radius and a sampling interval of 1 degree for the off-nadir angle. Then, based on the sampled user position, the corresponding signal propagation distance was calculated. Finally, based on (17)-(19) and the antenna pattern data in Figure 7, we calculated the carrier-to-noise ratio of the received signals for different users assuming that the receiving antenna gain is zero.

Fig. 8 shows the CNR of the navigation signals received by the user at different altitudes. It can be seen that the range of off-nadir angle of the navigation signal received by users of different heights is significantly different. When the height of the user is lower than the height of the navigation satellite, as the height of the user increases, the range of the off-nadir

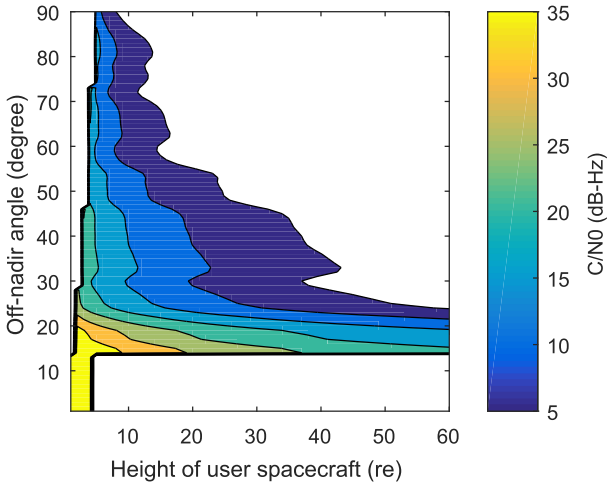

FIGURE 8. Carrier-noise ratio of the receiver of GPS as a function of the height of user spacecraft and off-nadir angle when the receiving antenna gain is 0 dB. The unit of the height of the user spacecraft is the radius of the earth.

angle of the available navigation signal becomes larger. When the height is far higher than the height of the navigation constellation, as the height of the user increases, the range of the available off-nadir angle of the navigation signal becomes smaller. For the user at the same height, except for a few angles, generally, the larger the off-nadir angle is, the lower the carrier-noise ratio is.

The range of the off-nadir angle of satellite signals received by the user on the surface of the earth generally does not exceed 14 degrees. Thus the horizontal orbital error contributes little to SISRE. As in Fig. 8, when the user height is lower than the navigation satellite height, the received signal is relatively strong, and the main factor affecting the coverage footprint is the geometric visibility. At this stage, the range of the off-nadir angle of the navigation signal received by the user satellite becomes larger, and the satellite coverage area also increases with the increase of the user height. When the user height is close to the navigation satellite height, the user can even receive a signal with a nadir angle greater than 80 degrees if the receiver is sensitive enough. With a larger nadir angle, the contribution of the horizontal orbit error to the SISRE became larger, and the participation of the radial orbit error to the SISRE became smaller. Thus, the weight factors of the along-track direction and cross direction orbit error should increase, and the weight factors of the radial direction orbit error should decrease at this stage. When the user height is higher than the navigation user height, the continuous attenuation of the signal strength makes it more and more challenging to receive a signal with a larger nadir angle. Then, the weight factors of the along-track direction and cross direction orbit error should begin to decrease, and the weight factors of the radial direction orbit error should increase as the user height increases.

C. WEIGHTING FACTORS OF TYPICAL SATELLITE NAVIGATION SYSTEM

As in Fig 8, the range of the off-nadir angle of the received navigation signal is a function of carrier-to-noise ratio thresholds. Since the scope of the off-nadir angle will affect the satellite coverage and the statistical value of SISRE, the statistical characteristic of SISRE under different carrier-to-noise ratio thresholds are also different. In the following analysis, we assumed that all the users are equipped with a multi-frequency, ultra-high sensitivity GNSS receiver with a 15 dB-Hz CNR threshold for space applications, as reported in [16]. Based on the analysis of the geometric visibility and the CNR threshold in the previous section, we obtained the coverage area of navigation satellite. Then, according to (8), we calculate the weighting factor of ephemeris error of different navigation satellites for the user at different heights.

Fig. 9 illustrates the trend of the weighting factor of GPS as a function of user height when the receiving antenna gain is 0 dB. It is evident that w_{A} equals to w_C, and they increase first and then decrease with the increase of user height. When the user height is 24000 km, w_{A} and w_C reach the maximum value of 0.276; in contrast, w_R and $w_{R,T}$ reduce first and then

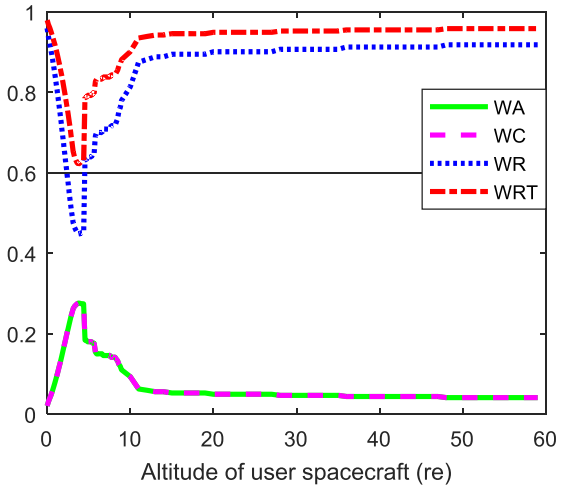

FIGURE 9. Global SISRE weight factors of GPS for the statistical contribution of radial (R) as well as along-track (A) and cross-track (C) errors when the receiving antenna gain is 0 dB. The unit of the height of the user spacecraft is the radius of the earth.

increase with the increase of satellite height. When the user height is 24000 km, w_R takes the minimum value of 0.448, and $w_{R,T}$ takes the minimum amount of 0.621.

Fig. 10 presents the trend of the weighting factor as a function of user height when the receiving antenna gain is 10 dB. It can be seen that with a higher antenna gain, the overall trend of the weighting factor does not change, but when the height of the user is higher than the navigation satellite, the rate of weighting factor variation is significant decreases. On the whole, the weighting factor of the radial orbit error decreases slightly, and the weighting factor of the horizontal orbital error slightly increases. When the user's orbital height is in the range of 26200-70000 km, w_{A} is maintained above 0.3. Thus, with the development of technology, high gain receiving antenna gain and high sensitivity receiver may make the horizontal orbit error contribute more and more to SISRE.

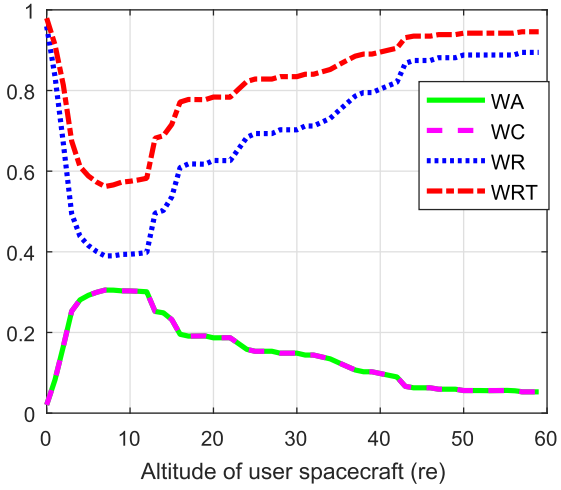

FIGURE 10. Global SISRE weight factors of GPS for the statistical contribution of radial (R) as well as along-track (A) and cross-track (C) errors when the receiving antenna gain is 10 dB. The unit of the height of the user spacecraft is the radius of the earth.

We summarized the weighting factor of different types of navigation satellites with a 0 dB receiving antenna gain in Figs. 11-13. It is clear that the variation trend of weighting factors of different navigation satellites is consistent. For GLONASS, GALILEO, Beidou MEO, and Beidou GEO, w_A reach the maximum value when the height of the user is about 47000 km, 38000 km, 32000 km, and 41000 km, respectively. It is evident that the user of GLONASS obtains the maximum w_A value at a higher height, for the transmitter power of GLONASS in the simulation is higher.

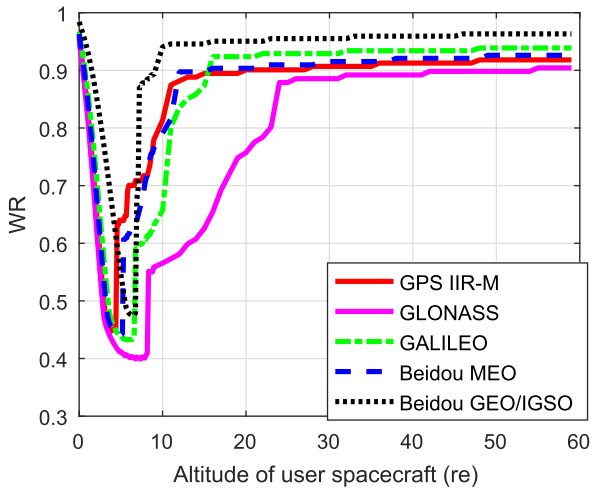

FIGURE 11. Global SISRE weight factors of typical navigation satellites for the statistical contribution of radial (R) errors when the receiving antenna gain is 0 dB The unit of the height of the user spacecraft is the radius of the earth.

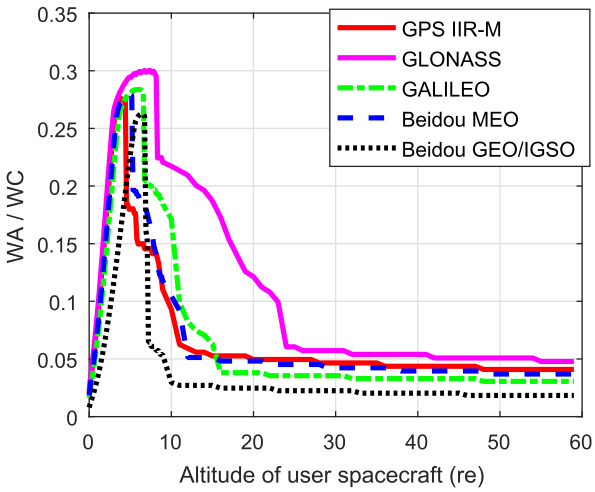

FIGURE 12. Global SISRE weight factors of typical navigation satellites for the statistical contribution of along-track (A) and cross-track (C) errors when the receiving antenna gain is 0 dB. The unit of the height of the user spacecraft is the radius of the earth.

IV. STATISTIC CHARACTERISTICS OF SISRE FOR SPACE USERS

As is mentioned before, SISRE is essentially a projection of ephemeris errors. Therefore, an accurate understanding of the characteristics of ephemeris errors is the basis for SISRE analysis.

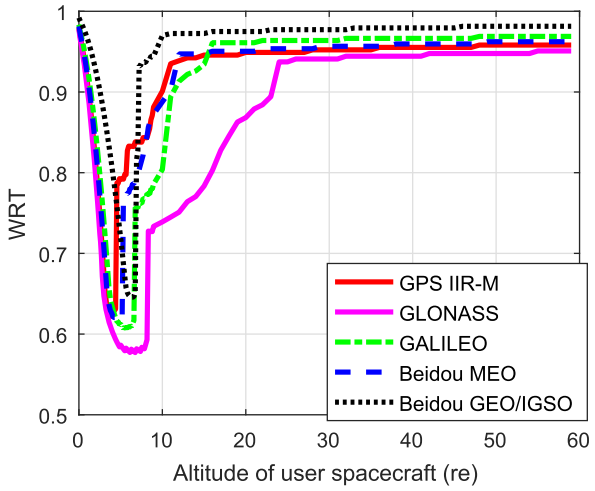

FIGURE 13. Global SISRE weight factors of typical navigation satellites for the statistical contribution of the correlation between the clock error and the radial orbit error when the receiving antenna gain is 0 dB. The unit of the height of the user spacecraft is the radius of the earth.

In principle, the difference between the broadcast and precise ephemerides can be used to calculate the orbit errors and clock errors and thus enables computation of the SISRE. The use of different conventions and pseudorange models in the two types of ephemerides requires careful consideration of antenna offsets corrections, time systems corrections, group delay corrections and, in some cases, relativistic time corrections [4]. The detail of the comparison has been described in [4]. Reference [1] summarized the accuracy of the broadcast ephemeris of existing navigation satellites but did not give the ephemeris accuracy of different types of satellites of Beidou individually. Therefore, as a supplement, we evaluated the accuracy of the Beidou satellite broadcast ephemeris from December 1st, 2018 to January 20th, 2019, to compare the ephemeris accuracy of different types of satellites of Beidou.

Based on the analysis results of the ephemeris error of Beidou (Fig. 14) and the ephemeris error data of other satellites in [1], we summarized the SISRE statistics of the typical navigation satellites in Table 2. Then, we substituted the ephemeris error statistics in Table 2 and the weighting factors given in Section III into (6) and (7) to obtain the statistics characteristic of SISRE of typical navigation satellites and summarized the results in Figs. 15-16 and Tables 3-4.

TABLE 2. RMS of ephemeris error of typical navigation satellites.

	R (m)	A (m)	C (m)	vT (m)	$\overline{\Delta t \Delta r}$ (m)
GPS IIR-M	0.18	1.05	0.44	0.69	0.13
GLONASS	0.35	2.41	1.33	1.9	0.01
GALILEO	0.63	2.65	2.29	1.62	0.26
Beidou MEO	0.74	2.59	1.12	1.14	1.28
Beidou GEO	0.88	6.25	2.26	0.73	0.71
Beidou IGSO	0.83	1.98	1.87	0.84	1.25

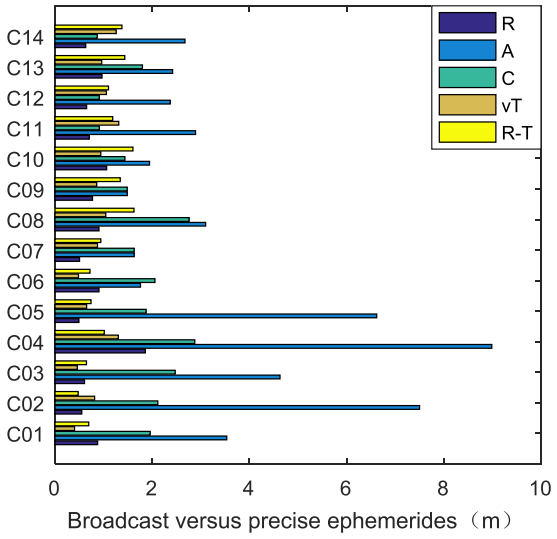

FIGURE 14. Root-mean-square orbit errors and clock errors of broadcast orbits relative to precise ephemerides of Beidou satellites. Here C01-C05 are GEO satellites, C06-C10 are IGSO satellites, C11-C14 are MEO satellites.

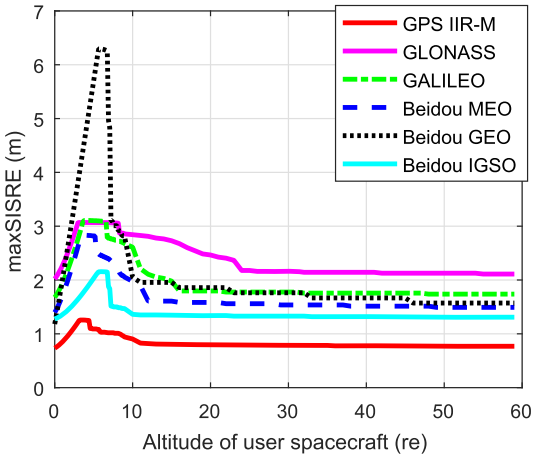

FIGURE 15. maxSISRE of typical navigation satellites for space users of different height when the receiving antenna gain is 0 dB. The unit of the height of the user spacecraft is the radius of the earth.

Figs. 15 and 16 show that the trends of maxSISRE and globalSISRE are the same as the trends of the weight factor of the along-track direction and cross direction orbit error, i.e., increase first and then decrease as the height of the user increases. When the user height is less than the navigation satellite height, with the value of the SISRE statistics of the terrestrial users as the baseline, the space user's SISRE generally increases due to the increased contribution of horizontal orbit error. When the orbit of the user is slightly higher than the navigation satellite, the SISRE takes the maximum value. Especially, for the Beidou GEO satellite, the mean of the along-track direction error is 6.25 meters, thus when the user height is about 42371 km, the maxSISRE can reach 6.30 m, far exceeding the ground user's 1.18 m. On the other hand, comparing Table 3 with Table 4, we can find that the increase of globalSISRE with the rise of the user height is much smaller than the rise in maxSISRE. For example,

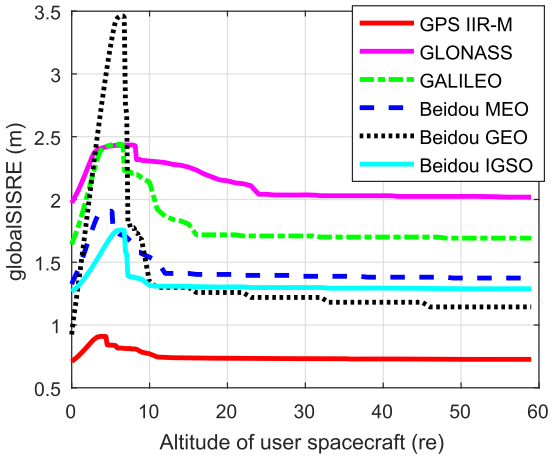

FIGURE 16. globalSISRE of typical navigation satellites for space users of different height when the receiving antenna gain is 0 dB. The unit of the height of the user spacecraft is the radius of the earth.

TABLE 3. maxSISRE of typical navigation satellites.

	Baseline (m)	Max value (m)	Growth rate (%)	Reference height (km)
GPS IIR-M	0.73	1.26	71	28371
GLONASS	2.02	3.07	52	26371
GALILEO	1.68	3.11	85	31371
Beidou MEO	1.40	2.83	103	30371
Beidou GEO	1.18	6.30	433	42371
Beidou IGSO	1.28	2.15	69	44371

TABLE 4. globalSISRE of typical navigation satellites.

	Baseline (m)	Max value (m)	Growth rate (%)	Reference height (km)
GPS IIR-M	0.71	0.91	28	30371
GLONASS	1.97	2.44	24	53371
GALILEO	1.64	2.44	49	44371
Beidou MEO	1.33	1.91	44	38371
Beidou GEO	0.92	3.46	275	47371
Beidou IGSO	1.27	1.76	39	47371

the globalSISRE of Beidou GEO increases by nearly 275%, and the maxSISRE of Beidou GEO increases by about 433% when the user height is approximately 47371 km and 42371 km respectively, compared with the user on earth. The difference between globalSISRE and maxSISRE of the SSV user is much more significant than the ground user; thus, SSV users generally cannot approximate maxSISRE with globalSISRE as ground users do. Moreover, a more substantial difference between globalSISRE and maxSISRE imply that the range of single-point SISRE of SSV user is larger than that of the ground user. This phenomenon not only amplifies the performance difference between different navigation systems but also makes the SISRE difference between the space user and different satellites of the same navigation system bigger.

V. CONCLUSION AND FUTURE WORK

SISRE is a key performance indicator for the comparison of different GNSS. This work focus on revealing the statistical characteristic of GNSS SISRE of user spacecraft. At first, based on the definition of SISRE, we derived the calculation

method of SISRE for space users. Then, we analyzed the geometric visibility and CNR of user spacecraft to obtain the relationship between the weighting factors of ephemeris errors and the orbital height of the user. Finally, we analyzed the statistics characteristic of SISRE of typical navigation satellites.

The analysis results show that SISRE of space users is related to various factors such as receiver sensitivity, antenna pattern, and user height. In general, SISRE of space user increases first and then decrease as the height of the user increases. For an SSV user, the contribution of the horizontal direction orbit error to the SISRE is significantly larger than the ground user and leads to a considerable increase in SISRE. Therefore, for satellites with large horizontal orbital errors, such as Beidou GEO, special attention should be paid to the variation of SISRE with orbital height. Besides, the range of single-point SISRE of SSV users is also larger than that of the ground user, and that amplifies the performance difference between different navigation satellites. In general, the maximum increase in maxSISRE for space users is approximately 52% to 433%, and the maximum increase for globalSISRE is approximately 24% to 275% compared to ground users.

For ground users, the GDOP is widely used as a criterion for selecting satellite, and the variances of range errors are assumed to be identical and independent distribution. However, this assumption contradicts the realistic environment because the performance difference of each measurement is more significant for an SSV user. Thus, we will try to use the weighted GDOP, instead of GDOP, in the future research about SSV to assess the performance of navigation and develop a reasonable satellite selection strategy.

REFERENCES

[1] O. Montenbruck, P. Steigenberger, and A. Hauschild, "Broadcast versus precise ephemerides: A multi-GNSS perspective," *GPS Solutions*, vol. 19, no. 2, pp. 321–333, Apr. 2015.

[2] L. Chen, W. Jiao, X. Huang, C. Geng, L. Ai, L. Lu, and Z. Hu, "Study on signal-in-space errors calculation method and statistical characterization of BeiDou navigation satellite system," in *Proc. China Satell. Navigat. Conf. (CSNC)*, 2013, pp. 423–434.

[3] L. Heng, G. X. Gao, T. Walter, and P. Enge, "Statistical characterization of GLONASS broadcast clock errors and signal-in-space errors," in *Proc. Int. Tech. Meeting Inst. Navigat.*, 2012, pp. 1697–1707.

[4] O. Montenbruck, P. Steigenberger, and A. Hauschild, "Multi-GNSS signal-in-space range error assessment—Methodology and results," *Adv. Space Res.*, vol. 61, no. 12, pp. 3020–3038, Jun. 2018.

[5] J. J. K. Parker, F. H. Bauer, B. W. Ashman, J. J. Miller, W. Enderle, and D. Blonski, "Development of an interoperable GNSS space service," in *Proc. 31st Int. Tech. Meeting Satell. Division Inst. Navigat. (ION GNSS)*, 2018, pp. 1246–1256.

[6] F. H. Bauer, J. Parker, B. Welch, and W. Enderle, "Developing a robust, interoperable GNSS space service volume (SSV) for the global space user community," in *Proc. Int. Tech. Meeting Inst. Navigat.*, 2018, pp. 132–149.

[7] A. Rathinam and A. G. Dempster, "Effective utilization of space service volume through combined GNSS," in *Proc. 29th Int. Tech. Meeting Satell. Division Inst. Navigat. (ION GNSS)*, Sep. 2016, pp. 223–227.

[8] Y. Tang, Y. Wang, and J. Chen, "The availability of space service for inter-satellite links in navigation constellations," *Sensors*, vol. 16, no. 8, p. 1327, Aug. 2016.

[9] E. Shehaj, V. Capuano, C. Botteron, P. Blunt, and P.-A. Farine, "GPS based navigation performance analysis within and beyond the space service volume for different transmitters' antenna patterns," *Aerospace*, vol. 4, no. 3, pp. 1–34, Aug. 2017.

[10] S. Jing, X. Zhan, J. Lu, S. Feng, and W. Y. Ochieng, "Characterisation of GNSS space service volume," *J. Navigat.*, vol. 68, no. 1, pp. 107–125, Jan. 2015.

[11] L. Heng, T. Walter, P. Enge, and G. X. Gao, "GNSS multipath and jamming mitigation using high-mask-angle antennas and multiple constellations," *IEEE Trans. Intell. Transp. Syst.*, vol. 16, no. 2, pp. 741–750, Apr. 2015.

[12] Y. Wu, X. Liu, W. Liu, J. Ren, Y. Lou, X. Dai, and X. Fang, "Long-term behavior and statistical characterization of BeiDou signal-in-space errors," *GPS Solut.*, vol. 21, no. 4, pp. 1907–1922, Sep. 2017.

[13] E. Kaplan and C. Hegarty, *Understanding GPS: Principles and Applications*, 2nd ed. Norwood, MA, USA: Artech House, 2005.

[14] B. W. Ashman, J. J. K. Parker, F. H. Bauer, and M. Esswein, "Exploring the limits of high altitude GPS for future lunar missions," in *Proc. 41st Annu. AAS Guid. Control Conf. (AAS/GNC)*, vol. 164, Feb. 2018, pp. 491–504.

[15] J. J. K. Parker, F. H. Bauer, B. W. Ashman, J. J. Miller, W. Enderle, and D. Blonski, "The multi-GNSS space service volume," in *Proc. 69th Int. Astron. Congr. (IAC)*, 2018, pp. 1–15.

[16] P. Blunt, C. Botteron, V. Capuano, S. Ghamari, M. Rico, and P. Farine, "Ultra-high sensitivity state-of-the-art receiver for space applications," in *Proc. 8th ESA Workshop Satell. Navigat. Technol. Eur. Workshop GNSS Signals Signal Process. (NAVITEC)*, Dec. 2016, pp. 1–8.

YIFAN ZHOU received the B.S. and M.S. degrees in instrument science and technology from the National University of Defense Technology, China, in 2013 and 2015, respectively, where he is currently pursuing the Ph.D. degree with the College of Intelligence Science and Technology. His research interests include GNSS, inter-satellite links, and autonomous orbit determination.

YUEKE WANG is currently a Professor with the College of Intelligence Science and Technology, National University of Defense Technology. His research interests include teaching and research in signal processing, space Instruments, and GNSS applications.

WENDE HUANG received the B.S., M.S., and Ph.D. degrees from the College of Mechatronics Engineering and Automation, National University of Defense Technology, China, in 2003, 2006, and 2011, respectively.

He is currently a Lecturer with the College of Intelligence Science and Technology, National University of Defense Technology. His research interests include orbit dynamics of spacecraft and satellite navigation technology.

LEYUAN SUN received the B.S. and M.S. degrees in aeronautics and space science and technology from the National University of Defense Technology, China, in 2014 and 2016, respectively, where he is currently pursuing the Ph.D. degree with the College of Intelligence Science and Technology.

His research interests include GNSS, inter-satellite links, and autonomous orbit determination.